

Fluorescence-ODMR of Light Harvesting Pigments of Photosynthetic Bacteria

A. Angerhofer, J. U. von Schütz, and H. C. Wolf

Physikalisches Institut, Teil 3, Universität Stuttgart, Pfaffenwaldring 57, D-7000 Stuttgart 80, Bundesrepublik Deutschland

Z. Naturforsch. **40c**, 379–387 (1985); received November 14, 1984/March 15, 1985

Light Harvesting Pigments, *Rhodospseudomonas sphaeroides*, Fluorescence-ODMR

Fluorescence detected ODMR measurements in zero field on the triplet states of light harvesting (LH) pigments in chromatophores from *Rhodospseudomonas sphaeroides* R 26.1 and *Rhodospseudomonas capsulata* $A1a^+$ are reported. In both cases at least two distinct triplet states in the antenna system with zfs values of D between 209 and 217 and E between 56 and $67 \times 10^{-4} \text{ cm}^{-1}$ are observed.

Introduction

The triplet state of photosynthetic pigments has been widely used in the past as an internal nondestructive probe for the geometric and electronic structure of the pigment-protein complexes of photosynthetic bacteria. Especially the reaction center complex (RC) has been intensively studied by means of ESR in high field and zero field [1–7]. Less is known about antenna complexes. So far only the light harvesting (LH) antenna complexes of the mutant $A1a^+ \text{ } pho^-$ from *Rhodospseudomonas* (*Rps*) *capsulata* [9] have been investigated by fluorescence detected magnetic resonance in zero magnetic field (F-ODMR) [8].

The LH antenna system of *Rps. sphaeroides* R 26.1 contains two subunits which are characterized by their different absorption, B 850 and B 870, which absorb at 850 nm and at 870 nm, respectively [10]. The minimal units of both types contain two different polypeptides each, the sequences of which have been analyzed recently [11]. It seems that ohne Bacteriochlorophyll molecule is bound to each polypeptide [12]. The LH antenna system of *Rps. capsulata* $A1a^+$ consists of one B 870 complex whose minimal unit is likewise formed by two polypeptides, the amino-acid sequences of which have been determined [13, 14].

In vivo these polypeptides aggregate with each other and with the reaction centers to form photosynthetic units in the chromatophore membranes. The red shift of the antenna bacteriochlorophyll absorption from 780 nm (*in vitro*) to 850 and 870 nm

seems to be due to the interaction of the pigments of at least 4 aggregated minimal units [15].

In the B 870 antenna complex from *Rps. capsulata* $A1a^+ \text{ } pho^-$, Beck *et al.* found 3 different triplet states by applying high resolution electron double resonance (EEDOR) [8].

In this contribution we want to report on the first F-ODMR experiments performed on the antenna system of the green mutants R 26.1 and $A1a^+$ from the purple photosynthetic bacteria *Rps. sphaeroides* and *Rps. capsulata*, respectively. The measurements were performed on chromatophores either oxidized with ferricyanide or treated with Triton TX 100 of low concentration. By this treatment we were able to get rid of the ODMR signal from the RCs which usually can be seen on the antenna emission band [16]. In both cases we could detect and coordinate the signals of more than one triplet state without the necessity to use high resolution EEDOR.

Materials and Methods

The chromatophores from *Rps. sphaeroides* R 26.1 and from *Rps. capsulata* $A1a^+$ were kind gifts from Prof. G. Drews, Freiburg. They were prepared in the usual way as described in [17]. The concentrated samples had an optical density (OD) of about 50 at the long wavelength maximum (1 cm cuvette).

Oxidation was performed by the addition of a 100 mM solution of potassium ferricyanide in tris buffer (pH 7.5) in equal proportion.

Detergent treated chromatophores were obtained by dropwise addition of 1% Triton TX 100 up to a final concentration of 1/2% in dim light at room temperature while stirring. These preparations were diluted in tris buffer (pH 7.9) and suspended in 70%

Reprint requests to Prof. Dr. H. C. Wolf

Verlag der Zeitschrift für Naturforschung, D-7400 Tübingen
0341–0382/85/0500–0379 \$ 01.30/0



Dieses Werk wurde im Jahr 2013 vom Verlag Zeitschrift für Naturforschung in Zusammenarbeit mit der Max-Planck-Gesellschaft zur Förderung der Wissenschaften e.V. digitalisiert und unter folgender Lizenz veröffentlicht: Creative Commons Namensnennung-Keine Bearbeitung 3.0 Deutschland Lizenz.

Zum 01.01.2015 ist eine Anpassung der Lizenzbedingungen (Entfall der Creative Commons Lizenzbedingung „Keine Bearbeitung“) beabsichtigt, um eine Nachnutzung auch im Rahmen zukünftiger wissenschaftlicher Nutzungsformen zu ermöglichen.

This work has been digitalized and published in 2013 by Verlag Zeitschrift für Naturforschung in cooperation with the Max Planck Society for the Advancement of Science under a Creative Commons Attribution-NoDerivs 3.0 Germany License.

On 01.01.2015 it is planned to change the License Conditions (the removal of the Creative Commons License condition “no derivative works”). This is to allow reuse in the area of future scientific usage.

glycerol to yield an OD of about 1 at the long wavelength maximum (1 cm cuvette). Samples for F-ODMR experiments were transferred to quartz tubes with 2 mm inner diameter and quickly frozen to liquid helium temperature. All samples were freshly prepared for each measuring period and kept on temperatures below 170 K during this time.

F-ODMR measurements were performed with the experimental setup shown in Fig. 1. The sample, cooled to 1.2 K in a homebuilt helium cryostat, was optically excited by an Argon dye laser system at the maximum of the BChl Q_x -transition at about 590 nm with light intensities between 200 and 500 mW. The fluorescence light was dispersed by a 0.5 m monochromator after passing 3 appropriate Schott RG filters in order to block the excitation light, and detected by a liquid nitrogen cooled photomultiplier with S1 cathode (EMI 9684). The amplified signal was digitized and processed by a HP 1000 MX computer. A microwave synthesizer (Ailtech 375), which was controlled by the computer, generated the microwaves which were amplified to about 100 mW by a Minicircuits ZHL 2-12 amplifier. The isolation between the RF-coil and the amplifier was performed by a directional coupler, the microwave power meas-

ured by a power meter (HP 435 A). The microwave spectrum could be analyzed by a spectrum analyzer (HP 8559 A). The computer controls the frequency sweeps of the synthesizer while averaging the recorded fluorescence signal.

Experimental Results

Fig. 2 A, B shows the fluorescence spectra of chromatophores from *Rps. sphaeroides* R 26.1 treated with ferricyanide and with TX 100, respectively. Both preparations have their long wavelength maximum at 903 nm in accordance with the emission of untreated chromatophores (data not shown). The spectrum of detergent treated chromatophores from *Rps. capsulata* A1a⁺ (Fig. 2C) shows its fluorescence maximum at 910 nm. It has an additional emission at 786 nm, which is also seen in the comparable preparations of *Rps. sphaeroides* R 26.1.

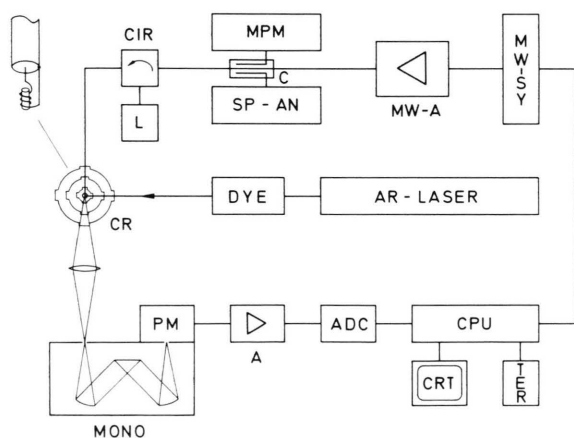


Fig. 1. Block-diagram of the experimental set-up with the following components:

MW-SY – microwave-synthesizer; MW-A – microwave-amplifier; MPM – microwave power meter; SP-AN – spectrum analyzer; C – coupler; L – load; CIR – circulator; CR – cryostat; A – picoampere-meter; ADC – analog-digital-converter; CPU – central processing unit; CRT – display; TER – terminal; MONO – monochromator; AR-Laser – Argon ion Laser; DYE – dye-laser; PM – photomultiplier.

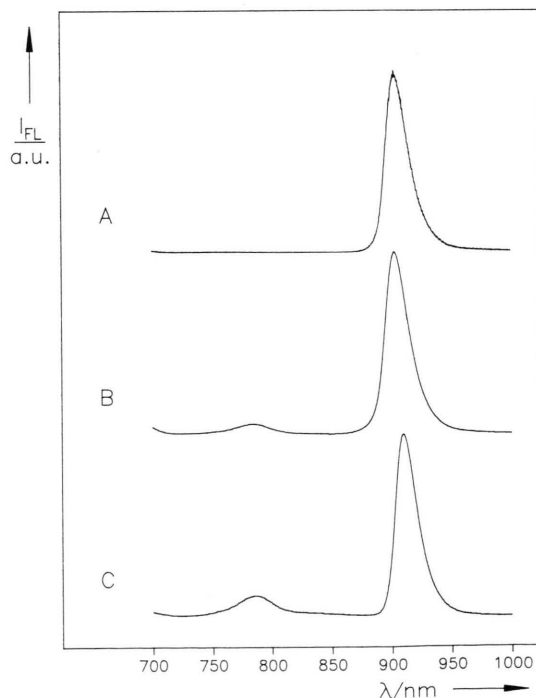


Fig. 2. Fluorescence emission spectra of different preparations at 1.2 K.

A: oxidized chromatophores of *Rps. sphaeroides* R 26.1
B: chromatophores of *Rps. sphaeroides* R 26.1 treated with 1/2% Triton TX 100.

C: chromatophores of *Rps. capsulata* A1a⁺ treated with 1/2% Triton TX 100.

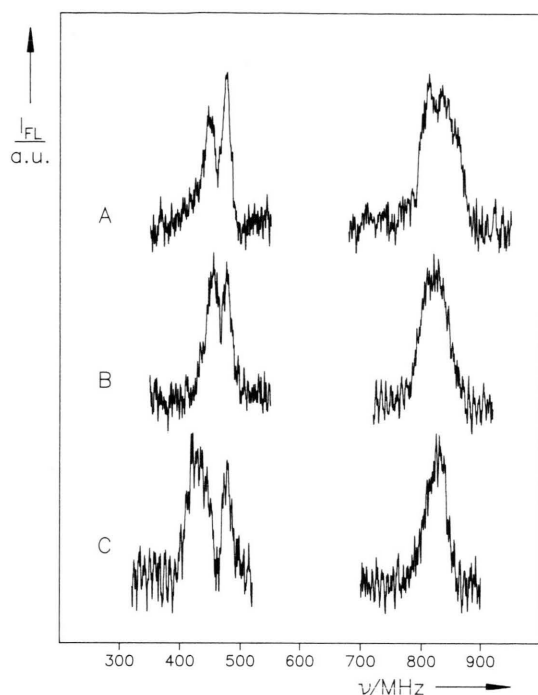


Fig. 3. F-ODMR spectra of different preparations at 1.2 K. A: oxidized chromatophores of *Rps. sphaeroides* R 26.1. B: chromatophores of *Rps. sphaeroides* R 26.1 treated with 1/2% Triton TX 100. C: chromatophores of *Rps. capsulata* Al α^+ treated with 1/2% Triton TX 100.

In Fig. 3 the F-ODMR spectra (transitions $D+E$ and $D-E$) of the same preparations are shown. They are monitored on the main emission maxima. The corresponding resonance frequencies are tabulated in Table I. Comparing the two different preparations of *Rps. sphaeroides* R 26.1, we find a good agreement between the spectral location of the three peaks. It should be noted that the relative intensities of the two maxima at 457 and 477 MHz vary for

Table I. The center frequencies of the F-ODMR signals from Fig. 3.

	Maximum frequencies [MHz]
R 26. 1. oxidized	455, 477, 812, 835
R 26.1 TX 100	457, 477, 820
Al α^+ TX 100	428, 476, 827

different samples. In accordance with this sample dependence, the shape of the $|D|+|E|$ -transition, centered at 820 MHz, shows small variations in bandwidth and frequency. In some cases two slightly resolved peaks at 812 and 835 MHz are visible on top of the band.

The variation of the F-ODMR signals as a function of the wavelength of detection is shown in Fig. 4 for chromatophores from *Rps. sphaeroides* R 26.1, treated by detergent. In the long wavelength tail of the emission (≥ 905 nm, Fig. 1) we find no variation in spectral location and relative intensities of the three resonance maxima. Going from 905 to 895 nm, however, we observe a decrease in intensity of the maximum at 477 MHz and a trend to asymmetry for the

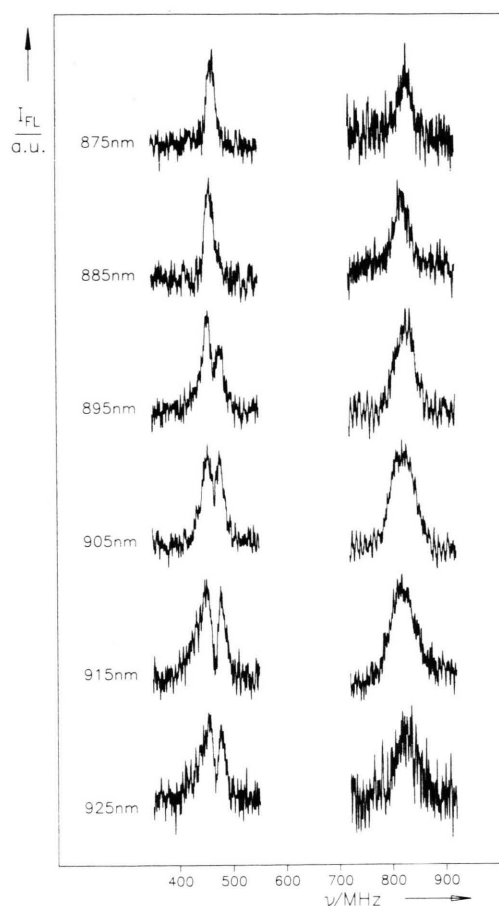


Fig. 4. Detection wavelength dependence of the F-ODMR spectra from Triton-treated chromatophores of *Rps. sphaeroides* R 26.1. The wavelength of detection is given on the left of the spectra.

820 MHz band with a new peak location at 832 MHz. By a further decrease of the wavelength of detection, the signal at 477 MHz fades away and the signal at 457 MHz shifts up to 467 MHz. A shift is also seen for the high frequency signal whose frequency is at 833 MHz when monitoring the fluorescence at 875 nm.

Fig. 5 shows the FMDR-signals detected using different microwave frequencies in the $|D| - |E|$ -region and the total emission spectrum for comparison. FMDR (Fluorescence-Microwave Double Resonance) means that one modulates the triplet state population of a fluorescing pigment species by a specific AM-modulated microwave frequency and uses the same modulation frequency for detection of the fluorescence spectrum via a lock-in [33]. In this way one gets only those fluorescence components of the total fluorescence spectrum which are influenced by the microwaves.

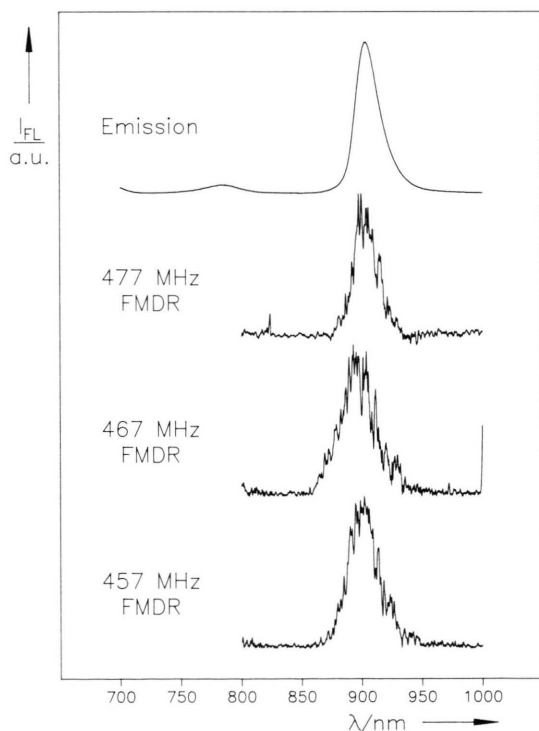


Fig. 5. Comparison between the FMDR-spectra of Triton-treated chromatophores of *Rps. sphaeroides* R 26.1 at various transition frequencies and the whole emission spectrum. The microwave frequencies are given on the left of the spectra.

The FMDR-spectra recorded using 457 and 477 MHz have their maximum at about 901 nm and are almost identical to the total emission spectrum, whereas the 467 MHz FMDR has its peak at 894 nm and contributes mainly to the short wavelength part of the total emission band.

In Fig. 6 the influence of high light intensity excitation (4 W Argon-Laser, all lines, 2 min, 1.2 K) is shown. After the illumination two negative signals at 465 MHz and 651 MHz appear additionally. The same holds for the samples treated by ferricyanide. These two lines correspond to the well known resonance frequencies of the intact reaction center which are observed with untreated chromatophores. We conclude that the chemical treatment can be at least partially reversed by the illumination.

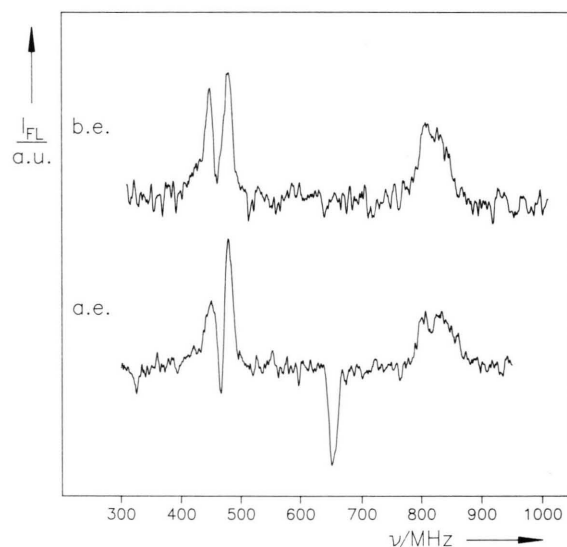


Fig. 6. Comparison of F-ODMR signals of Triton-treated chromatophores of *Rps. sphaeroides* R 26.1 before (b.e.) and after (a.e.) excitation with 4 W (Argon Laser all lines) for 2 minutes at a temperature of 1.2 K.

Discussion

Optical Spectra

The emission maxima at 903 nm for oxidized and detergent treated samples of *Rps. sphaeroides* R 26.1 have the same shape and spectral location as for the untreated chromatophores. The same is valid for *Rps. capsulata* Al⁺ whose chromatophores emit at

910 nm. These values are about 6 nm blueshifted as compared to the literature [18, 19]. This shift could be due to smaller optical densities of our samples causing minor reabsorption [20]. From excitation spectra (data not shown) it can be demonstrated that the observed fluorescence around 900 nm (Fig. 2) is due to the antenna pigments of the bacteria. This is the basis to ascribe the F-ODMR transitions to the antenna bacteriochlorophyll.

F-ODMR

For analysing the observed microwave resonance transitions we have to assume that two (or more) triplet states are involved. The $2|E\rangle$ -transition of bacteriochlorophyll *a* cannot be seen by conventional ODMR techniques [21].

The lack of the *negative* F-ODMR signal of the reaction centers at 660 MHz was considered as a proof that the concomitant *negative* RC-signal at 465 MHz is missing too and does not obscure the $|D\rangle - |E\rangle$ -signal of the antenna in this frequency region. Therefore we ascribe the two ODMR-signals at 457 and 477 MHz to the $|D\rangle - |E\rangle$ -transitions of two different antenna triplet states. The respective

$|D\rangle + |E\rangle$ -transitions overlap and form a broad, sometimes structured ODMR-signal between 800 and 850 MHz. We can coordinate the low frequency part of this band with its center at 812 MHz to the high frequency part of the $|D\rangle - |E\rangle$ -signals at 477 MHz. Consequently, the high frequency part of $|D\rangle + |E\rangle$ centered at 835 MHz belongs to the signal at 457 MHz. This could be proved further by careful examination of different samples which show different intensity ratios of both $|D\rangle - |E\rangle$ -signals and concomitant frequency shifts of the $|D\rangle + |E\rangle$ -signal.

Via the coordination mentioned above, the values of $|D\rangle$ and $|E\rangle$ can be calculated. In Table II they are compared with those from the B 870 antenna in *Rps. capsulata* $A1a^+ pho^-$ as well as with reaction centers and free bacteriochlorophyll in different solvents. Their values are between those of free bacteriochlorophyll *a* in various solvents and those detected in the antenna system of *Rps. capsulata* $A1a^+ pho^-$ and by far larger than those of RCs.

The observed reduction of $|D\rangle$ from 232 to $215 \times 10^{-4} \text{ cm}^{-1}$ (Table II) as compared with monomeric bacteriochlorophyll can be explained by the influence of selective spin orbit coupling [24, 25], provided that the red shift of the antenna absorption

Table II. Microwave resonance frequencies and $|D\rangle$ and $|E\rangle$ -values of antenna, reaction center and monomeric bacteriochlorophyll in various solvents.

	$ D\rangle - E\rangle$ [MHz]	$ D\rangle + E\rangle$ [MHz]	$2 E\rangle$ [MHz]	$ D\rangle$ 10^{-4} cm^{-1}	$ E\rangle$ 10^{-4} cm^{-1}	Ref.
B 870	459	782	323	207.0	53.9	[8]
<i>A1a^+ pho^-</i>	446	793	347	206.6	57.9	
	432	805	373	206.3	62.2	
B 870	476	(809)	—	214	56	this work
<i>A1a^+</i>	428	827	—	209.3	66.5	
B 870	I 477	812	—	215.0	55.9	this work
R 26.1	II 457	835	—	215.5	63.0	
*(875 nm)	III 467	833	—	216.8	61.0	
RC	467	657	190	187.5	31.7	[16]
R 26.1	463	678	215	190.3	35.9	
BC 780	490	901	—	232.0	68.5	
R 26.1						[7]
BChl <i>a</i> in MTHF	516	864	—	230.2	58.0	[21]
BChl <i>a</i> in THF				238	69	[22]
BChl <i>a</i> in tol/pyr				227	55	[23]

* (875 nm) means optical detection at 875 nm.

from 780 nm (free BCl in solution) to 840 nm (monomeric BCl in antenna systems [26, 27]) is due to a crystal field effect at the individual molecule's singlet state [7, 8]. From the crystal field shift of 920 cm^{-1} which is derived from the optical spectra in this way, we calculate a shift of the $|D|$ -value for the same system of $18 \times 10^{-4}\text{ cm}^{-1}$, if we use the empirical factor for porphyrins *in vivo*. In [7, 28] it has been shown that the relation between the zero field constant shifts and the optical transition shift is 0.06 MHz/cm^{-1} . Our measured $|D|$ -values are within this range of reduction. We can therefore neglect other $|D|$ -reducing effects like excitonic or CT-interactions between two bacteriochlorophylls in the triplet state for the interpretation of the $|D|$ -shift.

By observing the F-ODMR at shorter wavelengths (e.g. 875 nm), one finds another set of triplet state parameters which yields a slightly higher $|D|$ -value than the other antenna triplets (see Table II). However, it lies within the abovementioned range of antenna bacteriochlorophyll. By microwave modulated emission spectra (e.g. FMDR, see Fig. 5) the emission of only those pigments is recorded which are resonantly hit by the specific microwave frequency. The FMDR spectra recorded with the microwaves at 457 and 477 MHz are almost identical with each other and the total emission spectrum and therefore the pigments with triplets I and II contribute mainly to the total emission. Triplet III with its $|D| - |E|$ -frequency at 467 MHz and its FMDR-peak at 894 nm contributes mainly to the short wavelength part of the antenna emission.

As Cogdell pointed out [10], there exist two different antenna complexes in this bacterium called B 850 and B 870. They can be resolved spectrally by absorption spectroscopy below 100 K, whereas a resolution of the corresponding fluorescence maxima is not possible [18, 29]. Therefore we can only estimate values for the emission maxima of B 850 and B 870 by comparison with the fluorescence data of the antenna complex of the wild type strain *Rps. sphaeroides* 2.4.1. Wild type B 870 emits at 909 nm and wild type B 800–850 at 888 nm [18]. Because of effective energy transfer between B 800–850 and B 870, the emission at 888 nm is weak as compared with the emission at 909 nm.

Applying these feature to the case of strain R 26.1, B 850 emits at the short wavelengths region (around 890 nm) of the non-resolved total emission.

A finer resolution of the fluorescence can be

achieved by selective microwave excitation of different triplet states. Triplet III shows its FMDR spectrum with the maximum at 894 nm, whereas triplet I and II have their FMDR maxima at 901 nm.

So we tentatively ascribe triplet I and II to the B 870 complex and triplet III to the B 850 complex. The red shift of the FMDR spectrum of triplet III from 888 to 894 nm and the blue shift of the FMDR spectra from triplet I and II is easily explained by the fact that triplet I and II have contributions of their inhomogeneous line at 467 MHz, the resonance frequency of triplet III and *vice versa*. Therefore the superposition of the FMDR of B 870 (triplets I and II) and the FMDR of B 850 (triplet III) shifts both emissions towards each other. If this argumentation is correct, we find almost identical $|D|$ -values for B 850 and B 870 triplet states.

In order to explain the two different triplet states I and II, attributed to B 870, we recall that the smallest subunit of the B 870 type antenna in various species contains two bacteriochlorophyll molecules bound to two polypeptide chains [30–32]. The obvious assumption, is that the two different triplet states belong to these different pigment molecules. Their different geometrical arrangement within the protein could be the cause for slightly different triplet energies. Although this explanation seems reasonable, it is not able to account for the different intensity ratios between triplet I and II, found in different samples of the same species. The main difference in the zfs values of both triplets lies in the E-values which differ by 20% in their absolute value. Similar differences in $|E|$ are present in bacteriochlorophyll in different solvents (see Table II) which form pentacoordinate or hexacoordinate complexes with the pigments. Therefore we cannot exclude that the different triplet states arise from different coordination states of the antenna pigments.

The fact that the B 870 antenna of *Rps. capsulata* *Ala*⁺ shows two different triplet states as well, gives a hint that this is perhaps a basic feature of these kind of antenna pigments. In *Rps. capsulata* *Ala*⁺ *pho*[−] three different triplet states have been found by using high resolution EEDOR. Again the main difference in these states lies in the different $|E|$ -values. The fact that we observe in these systems several well defined slightly different triplet states is perhaps an indication that these multiple states are not artefacts due to the freezing process, a possibility which was discussed earlier [8].

Appendix

System and method: a short review about ODMR on photosynthetic bacteria.

1. Triplet-state finestructure

The level scheme in Fig. 7A (Jablonski diagram) containing the routes of excitation, shows that the lowest lying triplet state is populated via the optical excited S_1 -state by intersystem crossing. In nonsymmetrical molecules the triplet state splits into three sublevels even in zero external field (zero field splitting = zfs). This is caused by the spin-spin interaction of the unpaired electron spins [5]. The energy differences are measured by the triplet state finestructure parameters D and E . Plainly spoken D gives a measure for the delocalization of the triplet electrons

(spin-spin separation), whereas E measures the asymmetry of the electronic distribution within the molecular plane. Small deviations in molecular geometry or even in kind and geometry of the surrounding molecules will therefore influence D and E and can thus be detected. In our systems, D is in the order of $0.02 \text{ cm}^{-1} \approx 600 \text{ MHz}$ and E about $0.005 \text{ cm}^{-1} \approx 150 \text{ MHz}$.

2. ODMR (Optical Detected Magnetic Resonance)

By continuous light illumination of the sample, one finds a certain amount of molecules in the triplet state. Fortunately intersystem crossing rates to the different sublevels are not equal because of the different overlap integrals of the electronic wavefunctions of S_1 and τ_x, τ_y, τ_z . Therefore, if spin-lattice

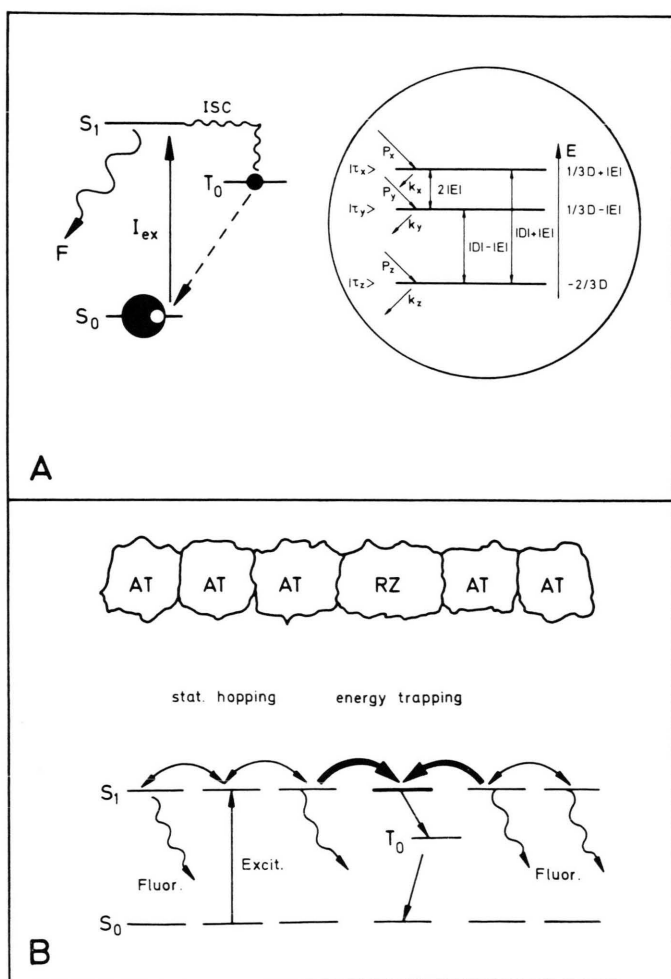


Fig. 7A. Level Scheme of an optically excited molecule, routes of excitations, intersystem crossing and depopulations as well as the dipolar splittings of triplet state in zero external field. B. Mutual arrangement of antenna complexes (AT) and reaction centers (RZ) which are populated via Förster-type energy transfer.

relaxation is slow against triplet decay, what is true at low temperatures, we obtain a considerable spin polarization in the triplet state (different occupation numbers). This is one basis for the detection of the microwave transitions. By resonant irradiation of a triplet spin transition *e.g.* $\langle \tau_x \rightarrow \tau_z \rangle$, the stationary occupation of the so combined levels is perturbed. The faster decaying level will either be overpopulated or underpopulated as long as the resonant microwaves are on. This results in an overall decrease or increase, respectively, of the triplet concentration and therefore in an increase or decrease of the fluorescence of the molecules. This method is therefore called F-ODMR (fluorescence-optically detected magnetic resonance).

3. EEDOR (Electron Electron Double Resonance)

If, under steady state conditions, two triplet levels *e.g.* τ_x and τ_y have nearly the same occupation number, microwave transitions will be invisible for normal ESR or ODMR. One has to saturate simultaneously another transition *e.g.* $\langle \tau_x \leftrightarrow \tau_z \rangle$ with cw microwave radiation in order to achieve a new steady state distribution of the triplet levels. τ_x will then equal its population with τ_z and differ from the population of τ_y . By irradiation with a second microwave source into the transition $\langle \tau_x \leftrightarrow \tau_y \rangle$ this difference will be detectable and the otherwise invisible resonance thus measurable.

4. FMDR (Fluorescence Microwave Double Resonance)

The resolution of superimposed optical spectra of different species by means of selective excitation and emission spectroscopy can be enhanced considerably by concomitant application of resonant microwave irradiation.

The microwave, fixed in frequency, is amplitude modulated; therefore those parts of a complex spectrum which belong to the triplet of resonance follow the modulation and can be recorded separately via a lock in amplifier locked upon the AM-frequency.

5. Signal shape analysis

The signals measured with ODMR techniques are usually inhomogeneous broadened lines, the homogeneous linewidth of which can be measured by hole burning experiments. *Shifts* in signal frequency

can therefore be interpreted as due to variations in the distribution of different sites. This can be correlated to shifts in the fluorescence maxima as well, so that each site has its own fine structure parameters and its own location of the fluorescence maximum. Correlating the triplet data to the singlet data in comparison with measurements *in vitro*, one can identify the different molecules within the sample via their triplet properties (see for example [7, 28]). The signal *amplitudes* normally reflect the spin polarization and thus the ratios of populating and depopulating kinetics of the triplet sublevels. Energy transfer between two molecular species, can be reflected by the ODMR signal signs also, as will be explained in the following.

6. Energy transfer in the chromatophores

Energy transfer in the chromatophore membrane takes place between antenna and reaction centers as is shown schematically in Fig. 7B. The reaction center is in this case no energetical trap but a diffusional trap. That means: Every time a reaction center is hit by an antenna exciton the energy is very quickly (few picoseconds) converted into an electron delocalization within the RC. Through reduction of the RC with sodium dithionite one can force the back reaction over the RC triplet state with a quantum yield of nearly 1 (low temperature case). Then microwave resonance in the RC triplet will strongly influence the number of "open" and "closed" traps (RC) and thus influence the fluorescence emission of the donor (AT). The ODMR signals of the RC triplet will therefore be visible on the fluorescence of the antenna but with amplitude reversed in sign. An increase in open traps (RC in the ground state) will increase RC fluorescence (positive signal) but decrease AT fluorescence (negative signal) which is the competitive process for trapping of excitons at the RCs. In order to view the AT triplet state one has to decouple the RC energetically from the AT system which can be done by oxidation or partial solubilization of the chromatophore membrane.

Acknowledgement

We thank Prof. G. Drews for the preparation of the chromatophores. We are very grateful to Dr. R. Cogdell for valuable discussion.

This work was supported by the "Deutsche Forschungsgemeinschaft".

- [1] J. D. McElroy, G. Feher, and D. C. Mauzerall, *Biochim. Biophys. Acta* **267**, 363 (1972).
- [2] D. M. Tiede, R. C. Prince, and P. L. Dutton, *Biochim. Biophys. Acta* **449**, 447 (1976).
- [3] R. H. Clarke and D. R. Hobart, *FEBS Letters* **82**, 155 (1977).
- [4] A. J. Hoff, *Physics Reports* **54**, 75 (1979).
- [5] A. J. Hoff in "Triplet State ODMR-Spectroscopy" (R. H. Clarke ed.) (1982) Chapter 9, p. 415/John Wiley and Sons, N. Y.
- [6] H. J. den Blanken, Dissertation, Rijksuniversiteit Leiden (1983).
- [7] J. Beck, Dissertation, Universität Stuttgart (1983).
- [8] J. Beck, J. U. von Schütz, and H. C. Wolf, *Chem. Phys. Lett.* **94**, 147 (1983).
- [9] G. Drews, P. Wevers, and R. Dierstein, *FEMS Microb. Lett.* **5**, 139 (1979).
- [10] E. Davidson and R. J. Cogdell, *FEBS Letters* **132**, 81 (1981).
- [11] R. Theiler, F. Suter, V. Wiemken, and H. Zuber, *Hoppe-Seyler's Z. Physiol. Chem.* **365**, 703 (1984).
- [12] R. Theiler and H. Zuber, *Hoppe-Seyler's Z. Physiol. Chem.* **365**, 721 (1984).
- [13] D. C. Youvan, M. Alberti, H. Begusch, E. J. Bylina, and J. E. Hearst, *Proc. Natl. Acad. Sci. USA* **81**, 189 (1984).
- [14] M. H. Tadros, F. Suter, H. H. Seydewitz, J. Witt, H. Zuber, and G. Drews, *Eur. J. Biochem.* **138**, 209 (1984).
- [15] P. Loach, S. Parkes and G. E. Gogel, Abstracts of the "Workshops on molecular structure and function of light-harvesting pigment-protein complexes and photosynthetic reaction centers", p. 52. 1983 in Zürich, Switzerland.
- [16] J. Beck, J. U. von Schütz, and H. C. Wolf, *Chem. Phys. Lett.* **94**, 141 (1983).
- [17] R. Dierstein and G. Drews, *Arch. Microbiol.* **106**, 227 (1975).
- [18] C. P. Rijgersberg, R. van Grondelle, and J. Ames, *Biochim. Biophys. Acta* **592**, 53 (1980).
- [19] R. Feick, R. van Grondelle, C. P. Rijgersberg, and G. Drews, *Biochim. Biophys. Acta* **593**, 241 (1980).
- [20] A. Angerhofer, Diplomarbeit, Universität Stuttgart (1982).
- [21] H. J. den Blanken and A. J. Hoff, *Chem. Phys. Lett.* **96**, 343 (1983).
- [22] R. H. Clarke, R. E. Connors, and H. A. Frank, *Biochem. Biophys. Res. Comm.* **71**, 671 (1976).
- [23] J. F. Kleibeuker, Dissertation, Landbouwhogeschool Wageningen (1977).
- [24] J. P. Lemaistre and A. H. Zewail, *Chem. Phys. Lett.* **68**, 296 (1979).
- [25] J. P. Lemaistre and A. H. Zewail, *Chem. Phys. Lett.* **68**, 302 (1979).
- [26] C. N. Rafferty, J. D. Bolt, K. Sauer, and R. K. Clayton, *Proc. Natl. Acad. Sci. USA* **76**, 4429 (1979).
- [27] V. A. Shuvalov and W. W. Parson, *Biochim. Biophys. Acta*, **638**, 50 (1981).
- [28] J. Beck, J. U. von Schütz, and H. C. Wolf, *Z. Naturforsch.* **38c**, 220 (1983).
- [29] J. D. Bolt and K. Sauer, *Biochim. Biophys. Acta* **637**, 342 (1981).
- [30] K. Sauer and L. A. Austin, *Biochemistry* **17**, 2011 (1978).
- [31] R. M. Broglie, C. N. Hunter, P. Delepelaire, R. A. Niederman, N.-H. Chua, and R. K. Clayton, *Proc. Natl. Acad. Sci. USA* **77**, 87 (1980).
- [32] R. Feick and G. Drews, *Biochim. Biophys. Acta* **501**, 499 (1978).
- [33] M. A. El Sayed, *MTP Int. Rev. Sci. Phys. Chem.*, Ser. 1, **Vol. 3**, p. 119, Butterworths, London 1972.